International Journal of Pharmaceutics 423 (2012) 184–194

Contents lists available at SciVerse ScienceDirect

International Journal of Pharmaceutics

journal homepage: www.elsevier.com/locate/ijpharm

Dry powder inhalers: Mechanistic evaluation of lactose formulations containing salbutamol sulphate

Waseem Kaialy[a,b], Martyn Ticehurst[c], Ali Nokhodchi[a,d,*]

[a] Chemistry and Drug Delivery Group, Medway School of Pharmacy, University of Kent, ME4 4TB Kent, UK
[b] Pharmaceutics and Pharmaceutical Technology Department, University of Damascus, Syria
[c] Pharmaceutical Sciences, PharmaTherapeutics, Pfizer, Sandwich, Kent CT13 9NJ, UK
[d] Drug Applied Research Center and Faculty of Pharmacy, Tabriz University of Medical Sciences, Tabriz, Iran

ARTICLE INFO

Article history:
Received 27 September 2011
Received in revised form 2 December 2011
Accepted 4 December 2011
Available online 17 December 2011

Keywords:
Inhalation
Commercial lactose
Salbutamol sulphate
Pulmonary delivery
Aerolizer®
Shape
Surface roughness
Content uniformity
Adhesion

ABSTRACT

The purpose of this study was to evaluate the relationships between physicochemical properties and aerosolisation performance of different grades of lactose. In order to get a wide range of physicochemical properties, various grades of lactose namely *Flowlac® 100* (FLO), *Lactopress anhydrous® 250* (LAC), *Cellactose® 80* (CEL), *Tablettose® 80* (TAB), and *Granulac® 200* (GRA) were used. The different lactose grades were carefully sieved to separate 63–90 μm particle size fractions and then characterised in terms of size, shape, density, flowability, and solid state. Formulations were prepared by blending each lactose with salbutamol sulphate (SS) at ratio of 67.5:1 (w/w), and then evaluated in terms of SS content uniformity, lactose–SS adhesion properties, and in vitro aerosolisation performance delivered from the Aerolizer®. Sieved lactose grades showed similar particle size distributions (PSDs) and good flow properties but different particle shape, particle surface texture, and particle solid state. Content uniformity assessments indicated that lactose particles with rougher surface produced improved SS homogeneity within DPI formulation powders. Lactose–SS adhesion assessments indicated that lactose particles with more elongated shape and the rougher surface showed smaller adhesion force between lactose and salbutamol sulphate. Lactose powders with higher bulk density and higher tap density produced smaller emission (EM) and higher drug loss (DL) of SS. In vitro aerosolisation for various lactose grades followed the following rank order in terms of deposition performance: GRA > TAB > LAC ≈ CEL > FLO. Linear relationships were established showing that in order to maximize SS delivery to lower airway regions, lactose particles with more elongated shape, more irregular shape, and rougher surface are preferred. Therefore, considerable improvement in DPI performance can be achieved by careful selection of grade of lactose included within DPI formulations.

1. Introduction

The respiratory tract is an attractive delivery route, with global drug delivery market size about 30% (Kaparissides et al., 2006). When considering pulmonary drug delivery, major advantages include avoiding the harsh conditions of the gastro intestinal, non-invasive route of administration, fast drug absorption and action, and local treatment of specific diseases (Wall, 1995). Dry powder inhalers (DPIs) are increasing in popularity for lung delivery due to their propellant free formulations and potentially rapid product development, making DPIs the most promising inhaler type for the future (Todo et al., 2001). With DPIs, the inhalable drug fraction is dependent on the inhaler device (Dalby et al., 1996), patient inhalation effort (Chan, 2006), and formulation properties (Kaialy et al., 2011a).

Carrier-drug based formulations are most commonly developed for delivery with DPIs (Telko and Hickey, 2005). Potential carriers for carrier-drug DPI formulations are somewhat limited because they have to meet strict toxicological standards. Carrier selection within DPI formulation is critical as carrier type has major effect on the DPI performance and an apparently minor change in carrier physicochemical properties could have a considerable effect of drug aerosolisation behaviour (Nokhodchi et al., 2011). Carrier particles should be selected based on their physicochemical properties such as size and morphology (Kaialy et al., 2011a), hygroscopicity (Harjunen et al., 2003), surface roughness (Kaialy et al., 2011b), and surface energy (Buckton, 1997).

Lactose is the most commonly used carrier in DPI formulations for pharmaceutical, physicochemical, and historical reasons. For example, lactose has both well documented stability and safety profiles (long track history of use in pharmaceutical formulations), can be produced by different manufacturing processes with predetermined properties, has high stability, low cost, and gives good flow properties (Smyth and Hickey, 2005). Lactose

* Corresponding author. Tel.: +44 1634 202947; fax: +44 1634 883927.
E-mail address: a.nokhodchi@kent.ac.uk (A. Nokhodchi).

0378-5173/$ – see front matter © 2011 Elsevier B.V. All rights reserved.
doi:10.1016/j.ijpharm.2011.12.018

exists in different forms including α-lactose monohydrate (Fries et al., 1971), α-lactose anhydrous (Platteau et al., 2005), β-lactose anhydrous (Hirotsu and Shimada, 1974), amorphous lactose (Roos and Karel, 1992), and anhydrous crystals with α and β lactose in different molar of ratios (Lefebvre et al., 2005). Different forms of lactose have different physical properties and different chemical stabilities. α-Lactose monohydrate is the natural, most stable, and the most commonly used DPI excipient (Nickerson, 1974) due to its less hygroscopic properties (Zeng et al., 2007). α-Lactose anhydrous is unstable (hygroscopic) (Briggner et al., 1994), difficult to obtain, and difficult to handle. β-Lactose is a stable anhydrous form, and has no tendency to form any hydrate phase. Spray dried lactose usually contains a mixture of α-lactose monohydrate particles and amorphous lactose. Molecular compounds of lactose have specific lattices resulting from association of α-lactose monohydrate and β-lactose with a hydrogen bonding. Lactose 5α/3β and lactose 3α/2β are the most common forms of molecular compounds of lactose (Drapier-Beche et al., 1999); yet, other forms can be formed depending on the operating techniques.

In literature, several reports showed that lactose aerosolisation performance was dependent on its physical prosperities. Different polymorphs of lactose produced dissimilar DPI performance due to their different physical and chemical properties (Traini et al., 2008). The formation of needle shaped lactose enhanced DPI performance (Larhrib et al., 2003) and has improved aerodynamic performance to penetrate deeper into the lung airways. Higher respirable drug fraction is generally obtained when fine particles are mixed with lactose coarse carrier particles (Kaialy et al., 2011c). More irregular shaped lactose particles with rougher surface produced enhanced DPI performance compared to commercial lactose product (Kaialy et al., 2011b,c). Electrostatic charge is believed to have considerable influence on drug detachment from carrier particles (Staniforth, 1996) and hence particle deposition on airway regions (Bailey et al., 1998; Hashish et al., 1998; Elajnaf et al., 2006). Interestingly, Chow et al. (2008) proved that the dynamic charge of lactose in influenced by the repeated inhaler use and increase with increasing relative humidity and aerosolization flow rate. A large number of lactose grades are commercially available with a wide range of physical properties. This gives the formulator a broad scope for the selection of the most suitable lactose material for a particular application. Although there is a substantial amount of scientific literature describing the role of lactose on DPI formulation performance there are only a handful of publications comparing the differences between commercial grades in depth and none of them, to best of our knowledge, compared different grades with similar particle size. Also, it is believed that this is the first study showing the DPI performance of *Cellactose*® (spray-dried product composed of 75% α-lactose monohydrate and 25% cellulose dry matter and designed originally for direct tableting). In the present paper, the influence of using different lactose grades [*Flowlac*® *100* (FLO), *Granulac*® *200* (GRA), *Tablettose*® *80* (TAB), *Cellactose*® *80* (CEL), and *Lactopress anhydrous*® 250 (LAC)] on inhalation properties of SS was investigated. By comparing these different lactose products, it will give formulators better understanding of the role of lactose physicochemical properties and DPI performance with readily obtainable materials.

2. Materials and methods

2.1. Materials

Flowlac® *100* (FLO) (spray dried α-lactose monohydrate), *Cellactose*® *80* (CEL) (spray dried: 75% α-lactose monohydrate and 25% cellulose), *Tablettose*® *80* (TAB) (agglomerated α-lactose monohydrate), and *Granulac*® *200* (GRA) (milled α-lactose monohydrate) were supplied from Meggle Group, Wasserburg, Germany. *Lactopress anhydrous*® 250 (LAC) (anhydrous β-lactose) was purchased from IMCD UK Limted. Micronised salbutamol sulphate (SS) ($D_{50\%} = 1.8 \pm 0.3$ μm, Kaialy et al., 2010a) was obtained from LB Bohle, Germany.

2.2. Sieving

All lactose powders were sieved to separate the 63–90 μm particle size (as precedent in the literature). Each lactose product powder was poured onto the top of 90 μm sieve (Retsch® GmbH Test Sieve, Germany) which was placed above another 63 μm sieve, and then the mechanical sieve shaker was operated for 30 min. After that, each 63–90 lactose particle size fraction was collected, placed on top of the 63 μm sieve, and subjected to air depression sieving (Copley Scientific, UK) at a gas volume flow that generates a negative pressure of 4 kPa for 15 min. After the sieving process was complete, the particles retained on the 63 μm sieve were collected and stored in sealed glass vials until required for further investigation. All experiments described below were carried out on the 63–90 μm particle size fractions.

2.3. Particle size distribution analysis

Particle size analysis was conducted using a Sympatec (Clausthal-Zellerfeld, Germany) laser diffraction particle size analyser as described in details previously (Kaialy et al., 2010b). Approximately 200–300 mg of the sample was dispersed in acetone and filled in cuvette. A test reference measurement was performed with the HELOS sensor using WINDOX software followed by a standard measurement. The particle size measurement was carried out under stirring condition during the experiment.

2.4. Image analysis optical microscopy

Quantitative particle shape analysis was performed using a computerized morphometric image analyzing system (Leica DMLA Microscope; Leica Microsystems Wetzlar GmbH, Wetzlar, Germany; Leica Q Win Standard Analyzing Software). For each lactose sample, a small amount of powder (about 20 mg) was dispersed on a microscope slide. The microscope slide was then manually tapped to remove accumulated powder until thin powder dust was homogenously scattered over the slide. For each lactose sample, minimum 350 particles were detected randomly from different positions and measured. Particle shape was assessed using several parameters including elongation ratio (ER) (Eq. (1)), flatness ratio (FR) (Eq. (2)), simplified shape factor (e_R) (Eq. (3)), and surface factor ($F_{surface}$) (Eq. (4)) (Kaialy et al., 2012; Kuo et al., 1998; Podczeck et al., 1999; Zeng et al., 2000):

$$\mathrm{ER} = \frac{\text{length}}{\text{breadth}} \tag{1}$$

$$\mathrm{FR} = \frac{\text{length}}{\text{breadth}} \tag{2}$$

$$e_R = \frac{\text{perimeter}_{\text{convex}}}{\text{perimeter}} - \sqrt{1 - \left(\frac{\text{breadth}}{\text{length}}\right)^2} \tag{3}$$

$$F_{\text{surface}} = F_{\text{shape}} \times \frac{(1+\mathrm{ER})^2}{\pi \times \mathrm{ER}} \tag{4}$$

where length is the maximum Feret diameter, breadth is the minimum Feret diameter (maximum and minimum Feret diameters were calculated from 16 Calliper measurements at 6° intervals around the particle), thickness is the Calliper diameter in the 90° direction, perimeter is the estimated perimeter of particle with

compensation for corners, and $\text{perimeter}_{\text{convex}}$ is perimeter of the minimum convex boundary circumscribing the particle.

2.5. Scanning electron microscope (SEM)

Electron micrographs of all lactose samples and lactose–SS formulations were obtained using a scanning electron microscope (Philips XL 20, Eindhoven, Netherlands) operating at 15 kV. The specimens were mounted on a metal stub with double-sided adhesive tape and coated under vacuum with gold in an argon atmosphere prior to observation. Different magnifications were used to observe the surface topography of different lactose particles.

2.6. Differential scanning calorimetry (DSC)

A differential scanning calorimeter (DSC7, Mettler Toledo, Switzerland) was used to characterise crystalline nature of different lactose samples. The equipment was calibrated using indium and zinc. Samples weighing between 4 mg and 5 mg were crimped and sealed nonhermetically in aluminium DSC pans with pin-hole lids. Each sample was heated from 25 °C to 300 °C at a scanning rate of 10 °C/min. A purge gas of nitrogen was passed over the pans with a flow rate of 50 mL/min. Different enthalpies were calculated by the software (Mettler, Switzerland).

2.7. Fourier transform infrared (FT-IR) spectroscopy

FT-IR were taken by FT-IR instrument (Perkin Elmer, USA) for different lactose samples at scanning range between 450 cm^{-1} and 4000 cm^{-1}. Each sample (several milligrams) was placed in the middle of the sample stage and a force applied (50 bar) using the top of the arm of the sample stage. After obtaining sharp peaks of appropriate intensity, the spectra acquired were the results of averaging four scans at 1 cm^{-1}.

2.8. True density measurements

The true density of all lactose samples was measured using an ultrapycnometer 1000 (Quantachrom, USA) using helium gas at an input gas pressure of 19 psi and an equilibrium time of 1 min.

2.9. Powder flow characterisation

Carr's index (CI) and angle of repose (α) were measured for all lactose powders as an indication of powder flowability. Each powder was filled into a 5 mL measuring cylinder and after recording the volume (bulk volume) the cylinder was tapped 100 times under ambient conditions (20 °C, 50% RH) and the new volume (tap volume) was recorded. The preliminary results showed that the use of 100 taps was sufficient to attain the minimum volume of the powder bed. Then, bulk density (D_b), tap density (D_t), Carr's Index (CI, Eq. (5)), and porosity (Eq. (6)) for each lactose sample was calculated using the following equations (Kaialy et al., 2011a):

$$\text{CI} = \left(\frac{D_t - D_b}{D_b}\right) \times 100 \tag{5}$$

$$\text{porosity} = \left(1 - \frac{D_b}{D_{\text{true}}}\right) \times 100 \tag{6}$$

Angle of repose was measured by the method adapted from (Kaialy et al., 2011a). In brief, a pile was built by dropping 1 g of each through a 75 mm flask on a flat surface. Angle of repose (α) was calculated using the following equation (where h is the height of the powder cone, and D the diameter of the base of the formed powder pile).

$$\tan\alpha = \frac{2h}{D} \tag{7}$$

2.10. Preparing carrier-drug formulations

SS was mixed separately with different sieved (63–90 μm) lactose powders in a ratio of (SS:lactose) 1:67.5 w/w (which is in accordance with the ratio used in commercial Ventolin™ Rotacaps™ (GSK)). This blending was carried out in cylindrical aluminium container (6.5 cm × 8 cm) using a Turbula® mixer (Willy A. Bachofen AG, Maschinenfabrik, Basel, Switzerland) at standard mixing conditions (100 rpm mixing speed and 30 min mixing time) for the preparation of all formulations. A total of 5 formulations with FLO, LAC, CEL, TAB, and GRA were prepared at constant conditions. After the blending process was complete, all formulations were stored in tightly sealed glass vials at least 24 h prior to any investigation.

2.11. Dose uniformity assessment

After preparing all formulations, drug content uniformity in each formulation was tested by taking a minimum of five randomly selected aliquots of sampled powder from different positions of formulation powder bed for assay of SS content. Each aliquot weighs 33 ± 1.5 mg corresponding to 481 ± 22 μg unit dose. Each sample was then dissolved in 100 mL distilled water contained in a volumetric flask and the amount of the active drug (SS) was determined using high performance liquid chromatography (HPLC) method as described elsewhere (Kaialy et al., 2010a). Average drug content for each formulation was expressed as the percentage of nominal SS unite dose (% uniformity, 481 ± 22 μg). The degree of SS content homogeneity within all formulations was expressed using coefficient of variation (% CV).

2.12. Evaluation of lactose–SS adhesion

Air depression sieving was employed to assess lactose–SS adhesion forces within formulations. A 45 μm sieve (Retsch® GmbhTest Sieve, Germany) was employed and the air jet sieving machine (Copley Scientific, Nottingham, UK) was operated at a gas volume flow that generates a negative pressure of 4 kPa. Accurately weight quantity of 1 g of each formulation was placed on top of the 45 μm sieve and minimum three samples (33 ± 1.5 mg corresponding to a unit SS dose: 481 ± 22 μg) were removed from different areas of each formulation after different functional sieving times (5 s, 10 s, 30 s, and 3 min). SS content in each formulation sample was quantified using HPLC and expressed as a percentage to the unite SS dose (481 μg). Adhesion assessments were conducted in an air-conditioned laboratory where the ambient temperature and relative humidity (RH) were 22 °C and 50%, respectively.

2.13. In vitro deposition study

After blending, each formulation was filled manually into hard gelatine capsules (size 3) with 33 ± 1.5 mg such that each capsule contained 481 ± 22 μg of SS. After filling, in order to allow any charge-relaxation to occur, capsules were stored in sealed glass vials for at least 24 h prior to any investigation. Deposition profiles of all formulations were assessed in vitro using Aerolizer® inhaler device and Multi Stage Liquid Impinger (MSLI) equipped with a USP induction port (IP) (Copley Scientific, Nottingham, UK). Pharmacopoeial deposition experiments were performed at flow rate that corresponds to a pressure drop of 4 kPa across the device (92 L/min),

as described in details elsewhere (Kaialy et al., 2010a). At flow rate of 92 L/min, MSLI effective cut-off diameters becomes as follows: stage 1 = 10.50 μm, stage 2 = 5.49 μm, stage 3 = 2.5 μm, and stage 4 = 1.37 μm. Each deposition experiment involved the aerosolisation of ten capsules and was repeated at least three times. Several parameters were employed to characterise the deposition profiles of the formulations under investigation including recovered dose (RD), emitted dose (ED), recovery (RE), emission (EM), mass median aerodynamic diameter (MMAD), and geometric standard deviation (GSD) which were calculated as described previously (Kaialy et al., 2010a).

Drug loss (DL) was defined as the percent ratio of amounts of SS remained in capsule shells plus I + M (inhaler + mouthpiece adapror) to the RD. Impaction loss (IL) was defined as the percent ratio of amounts of SS deposited on the IP plus MSLI stage 1 to the RD. Fine particle dose (FPD) (defined as amounts of SS with aerodynamic diameter ≤5.5 μm) was calculated as the sum of SS amounts deposited on MSLI stage 3 + stage 4 + filter. FPF was calculated as the percent ratio of FPD to RD. Effective inhalation index (EI) (Kaialy et al., 2011a) were calculated by Eq. (8):

$$EI = (EM \times FPF)^{1/2} \quad (8)$$

All aerosol deposition experiments were performed in an air-conditioned laboratory where the ambient temperature and relative humidity (RH) were 22 °C and 50% respectively.

2.14. Statistical analysis

One way analysis of variance (ANOVA) was applied to compare mean results in this study, with P values less than 0.05 being considered as indicative of significant difference. Where ANOVA indicated significant difference, Tukey's HSD post hoc test was applied. Multiple regression and correlation analysis were conducted using Microsoft Excel software (UK, 2007).

3. Results and discussion

3.1. Particle size measurements

In order to remove the influence of particle size and focus on other physical properties, only 63–90 μm sieved lactose particles were used in these studies. Particle size distribution (PSD) for all lactose powders were measured and shown in Fig. 1 along with volume mean diameter (VMD), volume specific surface area (SSA_v), and span. All sieved lactose powders showed similar VMDs (from 81.6 ± 2.6 μm to 84.9 ± 1.3 μm, $P > 0.05$) and ≤1% fine particles < 10 μm. This indicates that the sieving process was efficient and able to remove fine lactose particles adhering to the surface of larger lactose particles of all powders. Also, this is important in terms of limiting the effect of lactose particle size and lactose fines (<10 μm) on DPI performance. Regardless of lactose product type, the majority of lactose particles were between 52.6 ± 3.6 μm ($D_{10\%}$) and 117.8 ± 3.5 μm ($D_{90\%}$) in diameter. Nevertheless, specific surface area (SSA_v) and span between different lactose samples varied significantly (Fig. 1). FLO exhibited the lowest SSA_v (0.09 ± 0.02 m^2/cm^3) and lowest span (0.72 ± 0.01) whereas the highest SSA_v (0.15 ± 0.02 m^2/cm^3) and span (0.87 ± 0.09) values were seen with GRA (Fig. 1).

3.2. Particle shape characterisation

The shape of all lactose grades was quantitatively assessed using number of different shape descriptors based on image analysis optical microscopy including elongation ratio/flatness ratio (ER/FR), simplified shape factor (e_R), and surface factor ($F_{surface}$) which are

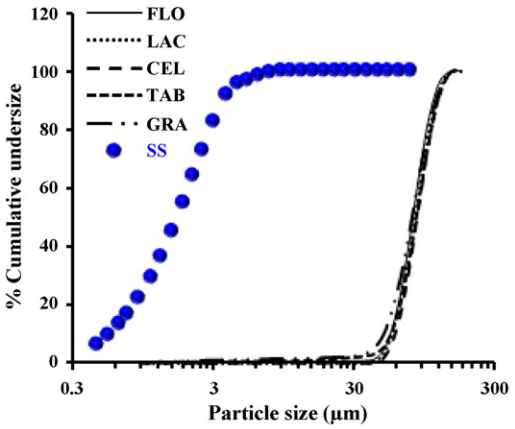

Lactose product	VMD (μm)	SSA_v (m^2/cm^3)	Span
FLO	81.6±0.9	0.09±0.02	0.72±0.01
LAC	81.9±1.4	0.10±0.02	0.80±0.02
CEL	84.9±1.3	0.13±0.03	0.82±0.05
TAB	82.6±3.2	0.14±0.01	0.86±0.08
GRA	81.6±2.6	0.15±0.02	0.87±0.09

Fig. 1. Percent cumulative undersize particle size distribution, volume mean diameter (VMD), volume specific surface area (SSA_v), and span for different 63–90 μm sieved lactose products: *Flowlac® 100* (FLO), *Lactopress anhydrous® 250* (LAC), *Cellactose® 80* (CEL), *Tablettose® 80* (TAB), and *Granulac® 200* (GRA) (mean ± SD, $n \geq 3$). (•) cumulative undersize particle size distribution for salbutamol sulphate (SS).

all displayed in Fig. 2. ER and FR are first order shape parameters which are considered the fundamental descriptors of particle shape (Kuo et al., 1998). Spheres and perfect cubes have ER and FR of 1.0. Higher ER is indicative of more elongated and/or more irregular shape whereas higher FR is indicative of more flattened shape. Higher ER/FR is indicative of more elongated/less flattened particle shape. e_R is a second order particle shape descriptor refers to particle shape irregularity (Podczeck and Newton, 1994). e_R can have values from −1 to 1 and smaller e_R values indicate greater shape irregularity and/or rougher particle surface. $F_{surface}$ is a third order shape descriptor refers only to particle surface roughness. Cubical particles with typical smooth surface are expected to have a $F_{surface}$ of 1 and particles with smaller $F_{surface}$ have rougher surface. Shape factors between different lactose carrier particles varied considerably as seen in Fig. 2. Differences in carrier particle shape might have considerable effect on DPI performance (Kaialy et al., 2011a, 2012).

Among all lactoses, FLO showed the lowest ER/FR (1.24 ± 0.01), the highest e_R (0.28 ± 0.01), and the highest $F_{surface}$ (0.86 ± 0.01) (Fig. 2) indicating that FLO particles have the least elongated and most regular shape and smoothest surface texture (closer to spheres with smoother surface). On the other hand, GRA showed the highest ER/FR (2.17 ± 0.01), the smallest e_R (−0.20 ± 0.00), and the smallest $F_{surface}$ (0.31 ± 0.00) (Fig. 2) indicating that GRA particles have the most elongated and most irregular shape and roughest surface topography.

Particle shape assessment using 2D image analysis is dependent on particle orientation and contact area with other particles which might affect the accuracy of the technique. Therefore, shape of all lactose particles was qualitatively explored using 3D scanning electron microscope (SEM) in the following section.

3.3. Scanning electron microscope (SEM) for different lactoses

SEM micrographs of different lactose particles are shown in Fig. 2. It can be observed that different lactose particles

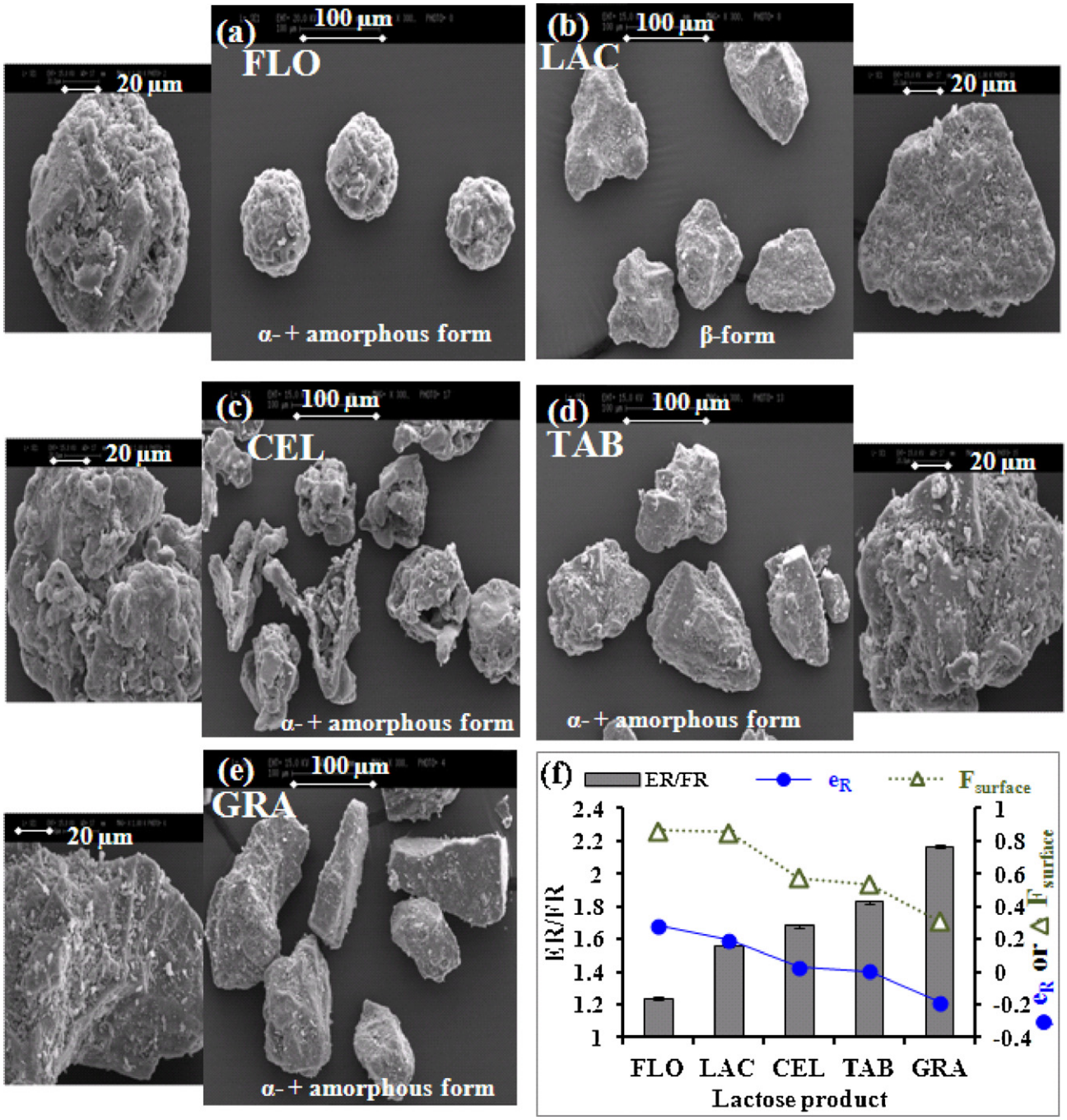

Fig. 2. Scanning electron micrographs (a–e) and different particle shape descriptors: (■) elongation ratio/flatness ratio (ER/FR), (•) simplified shape factor (e_R), and (Δ) surface factor ($F_{surface}$) **(f)** for different 63–90 µm sieved lactose powders: *Flowlac® 100* (FLO) **(a)**, *Lactopress anhydrousv® 250* (LAC) **(b)**, *Cellactose® 80* (CEL) **(c)**, *Tablettose® 80* (TAB) **(d)**, and *Granulac®200* (GRA) **(e)** (mean ± SE, $n \geq 350$).

showed similar mean sizes but distinctly different morphologies which is in agreement with PSD and image analysis data (Figs. 1 and 2). FLO particles were rounded (spherical) particles with smoothly curved sides. CEL particles were observed as sub-rounded particles having nearly plane sides, well-rounded corners and edges, and visible pores and cavities on the surface. Also, un-crystalline "amorphous" regions could be clearly observed in case of FLO and CEL (glassy surface texture). LAC particles showed a kite-like shape while TAB sample appeared as triangular-subangular particles with few edges. GRA was visualized as angular elongated particles with sharp edges and rough surfaces. 3D SEM observations were in accordance with 2D image analysis confirming that FLO particles have the most spherical and most regular shape among all lactoses whereas GRA particles have the most elongated and most irregular shape.

3.4. Solid state characterisation

Thermal transitions of all lactose particles were detected using DSC and all traces with transition enthalpies are given in Fig. 3a. FLO, GRA, TAB, and CEL showed the typical DSC thermal trace of α-lactose monohydrate having two distinctive endothermic transitions at 148.1 ± 0.3 °C (corresponding to crystalline water dehydration) and 216.0 ± 1.2 °C (corresponding to α-lactose melting), and one exothermic transition at 177.0 ± 0.3 °C

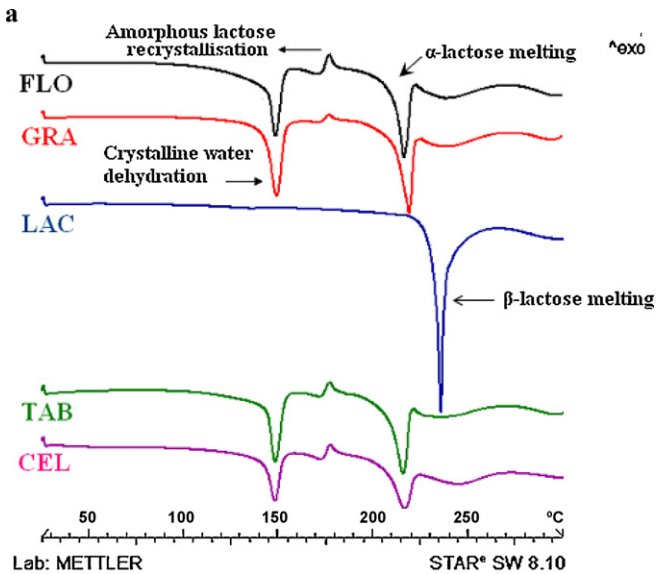

Lactose product	ΔHv (J/g)	Δhc (J/g)	ΔH_{216} (J/g)	ΔH_{234} (J/g)
FLO	100.7±5.3	21.2±1.8	115.8±1.8	…
GRA	115.9±3.1	9.0±2.1	124.0±4.5	…
LAC	…	…	…	275.1±4.5
TAB	94.4±0.4	17.9±0.9	114.6±0.8	…
CEL	68.0±0.8	20.1±2.5	77.4±1.8	…

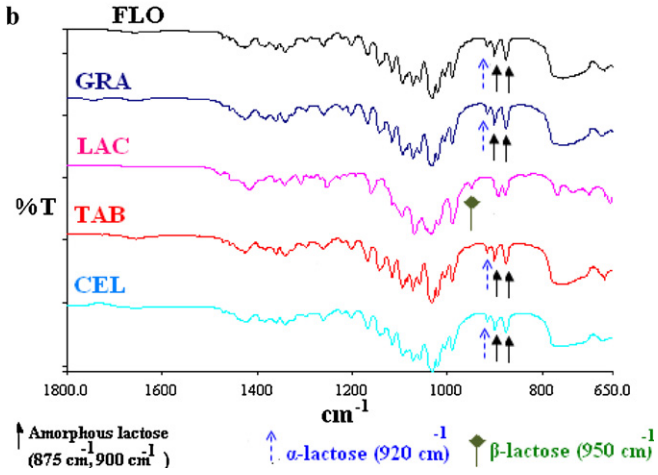

Fig. 3. **(a)**DSC thermal traces, crystalline water dehydration enthalpy (ΔH_v), amorphous lactose recrystallisation enthalpy (ΔH_c), α-lactose melting enthalpy (ΔH_{216}), β-lactose melting enthalpy (ΔH_{234}) (mean ± SD, $n = 3$); **(b)** FT-IR spectra for different 63–90 μm sieved lactose products: *Flowlac® 100* (FLO), *Granulac®200* (GRA), *Lactopress anhydrous® 250* (LAC), *Tablettose®80* (TAB), and *Cellactose®80* (CEL).

(corresponding to amorphous lactose recrystallisation) (Kaialy et al., 2011a,b) (Fig. 3a). The subsequent events for all samples could be related to thermal degradation of different products. LAC showed the typical DSC thermal trace of β-lactose with distinctive β-lactose melting transition at 233.9 ± 0.3 °C (Kaialy et al., 2011a,b). No endothermic transitions were detected bellow 100 °C for all samples (Fig. 3a) suggesting that none of the lactose grades contain significant amounts of free water (surface water).

A linear relationship ($r^2 = 0.9287$) was obtained when plotting crystalline water dehydration enthalpy (ΔH_v) against α-lactose melting enthalpy (ΔH_{216}) of different lactose products (Figure not shown), which was expected since α-lactose exists as monohydrate form. GRA showed the smallest amorphous lactose recrystallisation enthalpy (ΔH_c) (9.0 ± 2.1 J/g) indicating lowest amorphous lactose content whereas highest ΔH_c enthalpy were obtained from FLO (21.2 ± 1.8 J/g) and CEL (2.1 ± 2.5 J/g) products showed the which is indicative of highest amorphous lactose content (Fig. 3a).

Fourier transform infrared (FT-IR) spectra were used to investigate differences in lactose samples on molecular level and all spectra are shown in Fig. 3b. FLO, CEL, TAB, and GRA showed the reference spectrum of α-lactose monohydrate having a specific diagnostic band at 920 cm^{-1} whereas LAC showed the reference spectrum of β-lactose with specific diagnostic band at 950 cm^{-1} (Kaialy et al., 2011a,b). Absorptions at 1260 cm^{-1} and 900 cm^{-1} were observed in case of FLO, CEL, TAB, and GRA samples which is indicative of the presence of amorphous lactose (Kaialy et al., 2011a,b). FT-IR results were supportive to DSC results showing that LAC was in pure β-lactose form whereas FLO, CEL, TAB, and GRA were in α-lactose monohydrate form with varying degrees of crystallinity.

3.5. Density and flowability measurements

True density (D_{true}), bulk density (D_b), tap density (D_t), Carr's index (CI), angle of repose (α), and porosity for all lactose products are listed in Table 1. All lactose samples showed identical D_{true} (1.55 ± 0.01 g/cm^3) with the exception of LAC that have higher D_{true} (1.59 ± 0.01 g/cm^3) (Table 1). Different D_{true} for LAC are attributed to its different crystalline nature (β-lactose form) compared to FLO, CEL, TAB, and GRA (α-lactose form) as discussed previously in solid state section, as it is known that different lactose forms have considerably different true densities (Kaialy et al., 2011c). Lactose powders showed dissimilar D_b, D_t, CI, α, and porosity (Table 1). Direct linear proportionality ($r^2 = 0.9768$) was found between CI and α showing good agreement between the two methods (figure not shown). Both CI and α data indicated good flow character of all lactose products, which is needed to achieve satisfactory DPI formulation metering, fluidization, and dispersion (Taylor et al., 2000).

By comparing different lactose powders, CEL showed the lowest D_b (0.49 ± 0.00 g/cm^3), the lowest D_t (0.56 ±0.01 g/cm^3), and the highest porosity (68.2 ± 0.0%) whereas GRA showed the highest D_b (0.70 ± 0.00 g/cm^3), the highest D_t (0.82 ± 0.00 g/cm^3), and the lowest porosity (54.4 ± 0.0%) (Table 1). This indicates that, contrary to GRA, CEL powder has the lowest cohesiveness properties and lowest interparticulate forces. This could be attributed to spherical particle shape (Fig. 2) in case of CEL, which is likely to lead to increased void space between particles.

3.6. Evaluation of lactose–SS formulations

3.6.1. Scanning electron microscope for different formulations

SS alone powder showed particles less than 5 μm in size with typical rectangular shape (Fig. 4). These particles exist as polydisperse particles with apparent degree of aggregation. Visual examination of particle morphology showed that all lactose particles have a rough granular surface texture. Inspection of SEM images for lactose–SS formulations using high magnifications (3000×) revealed SS particles adhered to lactose surfaces as individual particles (Fig. 4) confirming the formation of lactose–SS interactive mixtures suitable for DPIs. It can be suggested that, during mixing, agglomerations formed from only drug–drug particles are likely to de-agglomerate by impaction with lactose carrier particles and blending vessel walls (de Villiers, 1997).

3.6.2. Homogeneity test

It is known that homogenous drug content is essential to achieve uniform metering doses by the patient during inhalation. Therefore, potency (% nominal dose) and coefficient of variation (% CV) for all formulations under investigation were assessed and shown

Table 1
True density (D_{true}), bulk density (D_b), tap density (D_t), Carr's index (CI), angle of repose (α), and porosity for different 63–90 μm sieved lactose products: *Flowlac® 100* (FLO), *Lactopress anhydrous® 250* (LAC), *Cellactose® 80* (CEL), *Tablettose® 80* (TAB), and *Granulac® 200* (GRA) (mean ± SD, $n \geq 6$).

	D_{true} (g/cm^3)	D_b (g/cm^3)	D_t (g/cm^3)	CI (%)	α (°)	Porosity (%)
FLO	1.55 ± 0.01	0.61 ± 0.01	0.69 ± 0.00	11.6 ± 1.2	25.1 ± 1.0	60.8 ± 0.0
LAC	1.59 ± 0.01	0.67 ± 0.00	0.78 ± 0.00	14.2 ± 0.3	28.2 ± 1.0	58.0 ± 0.0
CEL	1.55 ± 0.00	0.49 ± 0.00	0.56 ± 0.01	12.0 ± 0.8	26.1 ± 1.8	68.2 ± 0.0
TAB	1.55 ± 0.01	0.62 ± 0.01	0.73 ± 0.00	15.5 ± 0.5	29.6 ± 1.0	60.1 ± 0.0
GRA	1.55 ± 0.00	0.70 ± 0.00	0.82 ± 0.00	13.8 ± 0.4	28.2 ± 0.4	54.4 ± 0.0

in Fig. 5. Different formulations showed substantially different % potencies ranging from 75.4 ± 3.2% for CEL-SS formulation to 85.3 ± 3.3% for TAB-SS formulation and different % content homogeneity (expressed as % CV) (ranging from CV = 1.9% for GRA-SS formulation to CV = 9.0% for LAC-SS formulation) (Fig. 5a). Smallest % CV (1.9%) was obtained from GRA-SS formulation which is indicative of best SS content homogeneity among all formulations (Fig. 5a). On the other hand, FLO-SS and LAC-SS formulations produced the highest %CVs (8.3% and 9% respectively) indicating poorest SS content homogeneity (Fig. 5a). By comparison, direct linear relationship ($r^2 = 0.9701$) was obtained when plotting %CV of SS against lactose $F_{surface}$ indicating improved SS content homogeneity for formulations containing lactose particles with rougher surface (Fig. 5b). This outcome was supportive of previous studies where lactose particles with rougher surface generated formulations with better content uniformity for terbutaline sulphate (Flament et al., 2004) and salbutamol sulphate (Kaialy et al., 2011b). For comparison purpose, which is intended in this study, all formulations were blended at the same standard conditions without optimization for each type of powder.

3.6.3. Lactose–SS adhesion assessment

Lactose–SS adhesion characteristics within all formulations were evaluated by air jet sieving, upon which, small SS particles are promoted to detach from coarse lactose surfaces. Amounts of SS (%, nominal dose) collected after different functional sieving times from all formulations are illustrated in Fig. 6a. Assuming particle adhesion force is equivalent to particle detachment force, smaller amounts of SS remained after sieving indicates weaker lactose–SS adhesion forces. It can be seen that, for all formulations, amounts of SS decreased as sieving time increased (Fig. 6a) confirming that all formulations were order mixtures. Among all lactose products, GRA produced the lowest amounts of SS after all functional sieving times (43.6 ± 1.1%, 20.4 ± 0.4%, 13.5 ± 1.7%, 10.9 ± 0.5% after 5 s, 30 s, 1 min, and 3 min functional sieving time respectively) indicating that GRA-SS formulation has the lowest lactose–SS adhesion forces (Fig. 6a). Differences in lactose–SS adhesion forces between different formulations could be attributed to different physical properties of lactose products included as the same batch of SS, the same lactose–SS ratio, and same blending conditions were used in preparation of all formulations. Fig. 6b shows that lactose particles

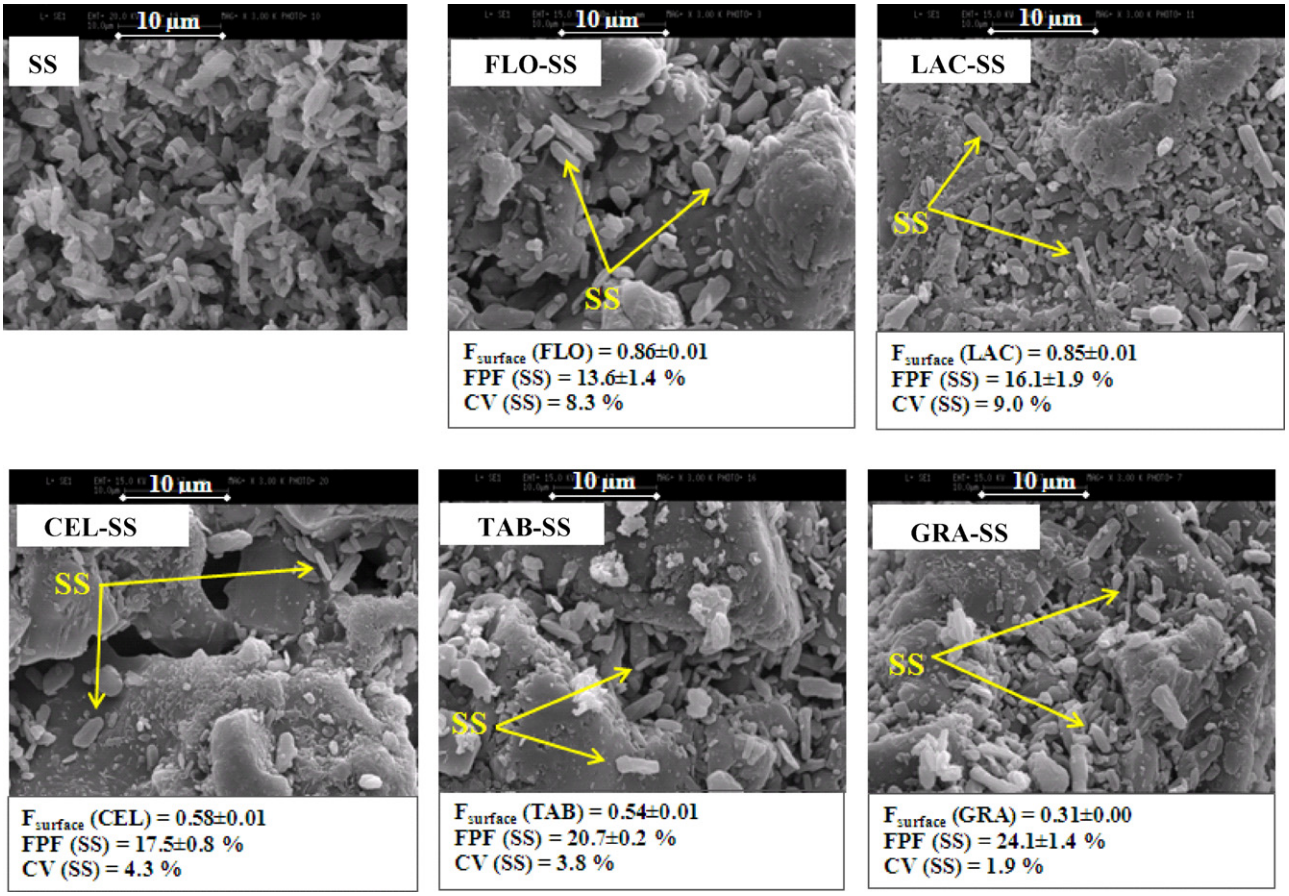

Fig. 4. SE micrographs for salbutamol sulphate (SS) alone and lactose–SS blends using different 63–90 μm sieved lactose products: *Flowlac® 100* (FLO), *Lactopress anhydrous® 250* (LAC), *Cellactose® 80* (CEL), *Tablettose® 80* (TAB), and *Granulac® 200* (GRA).

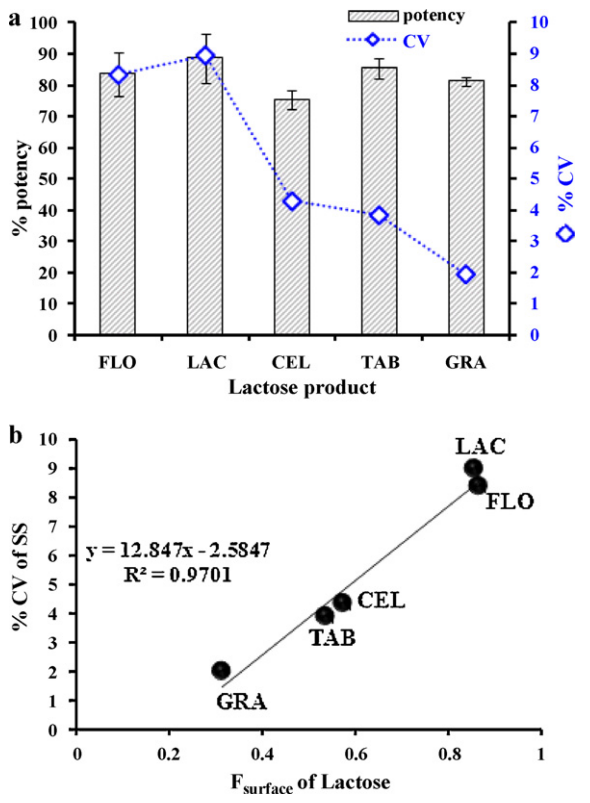

Fig. 5. **(a)** ▨ Percent uniformity (mean ± SD, $n \geq 5$) and (◊) coefficient of variation (% CV) of salbutamol sulphate (SS) content; **(b)** (●) relationship between % CV of SS and surface factor ($F_{surface}$) of lactose (mean ± SE, $n \geq 350$) obtained from formulations containing different 63–90 μm sieved lactose products: *Flowlac® 100* (FLO), *Lactopress anhydrous® 250* (LAC), *Cellactose® 80* (CEL), *Tablettose® 80* (TAB), and *Granulac® 200* (GRA).

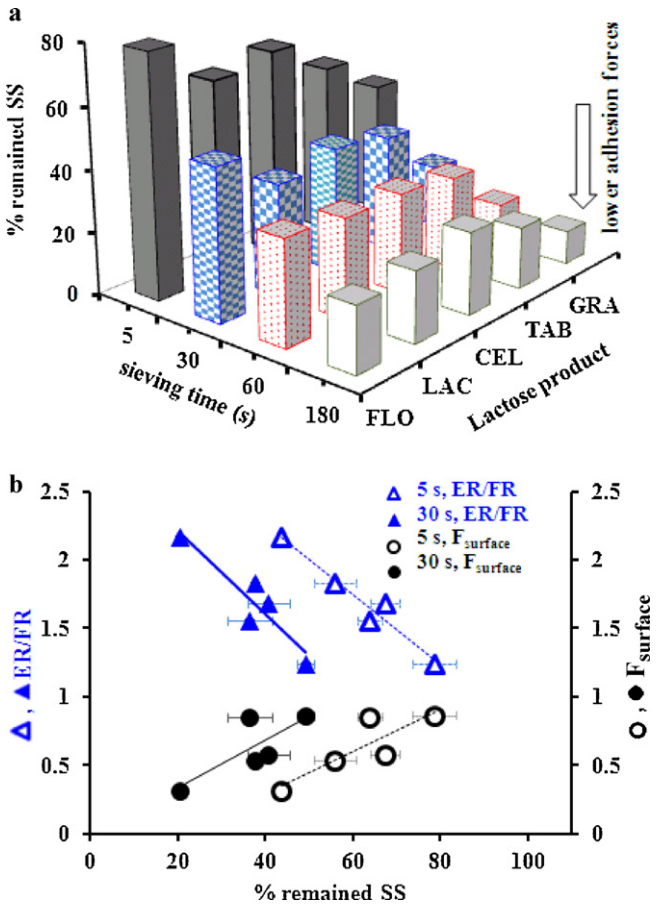

Fig. 6. **(a)** Remained salbutamol sulphate (SS) (%, 481 μg) (mean ± SD, $n \geq 3$) after subjecting different lactose–SS blends to different functional sieving times; **(b)** % remained SS after 5 s or 30 s sieving time in relation to surface factor ($F_{surface}$) and elongation ratio/flatness ratio (**ER/FR**) of different lactose particles: *Flowlac® 100* (FLO), *Lactopress anhydrous® 250* (LAC), *Cellactose® 80* (CEL), *Tablettose® 80* (TAB), and *Granulac® 200* (GRA).

with rougher surface (smaller $F_{surface}$) and more elongated shape (higher ER/FR) produced smaller amounts of SS remained on 45 μm sieve indicating smaller lactose–SS adhesion forces. This could be ascribed to decreased lactose–SS contact area in case of lactose particles with more elongated shape and rougher surface.

3.6.4. *In vitro deposition test*

Mass distribution and aerodynamic particle size distribution of SS obtained from formulations containing different lactose products are shown in Fig. 7a and b.It can be seen amounts of SS remained in capsule shells and I + M from different formulations varied considerably (the highest amounts were produced by GRA: 6.9 ± 0.3% (Fig. 7a)). In fact, it can be assumed that drug particles separate from carrier particles even within the capsules and hence deposit on capsule walls. Amounts of SS deposited on throat (IP) were not influenced considerably ($P > 0.05$, 2.6 ± 0.9%) by using different lactose products. All formulations produced maximal deposition of SS on MSLI stage 1 (Fig. 7a). By comparison, GRA produced the lowest deposition of SS on MSLI stage 1 (48.8 ± 0.3%) and the highest deposition of SS on MSLI stage 4 (16.2 ± 0.8%) and filter (4.1 ± 0.5%) whereas FLO produced the highest deposition of SS on MSLI stage 1 (77.9 ± 1.9%) and the lowest deposition of SS on MSLI stage 4 (5.6 ± 0.7%) and filter (1.3 ± 0.3%) (Fig. 7a). Fig. 7b shows that the cumulative amounts of SS with aerodynamic diameter ≤10.5 μm, ≤5.5 μm, and ≤2.5 μm were dependent on lactose type product included in each formulation by the following order: GRA > TAB > LAC ≈ CEL > FLO. These results point out that GRA produced the highest amounts of SS deposited on lower airway regions whereas FLO produced the smallest amounts. Generally and for asthma therapy, optimal drug delivery requires that higher amount of drug delivered to the lung (which is the target organ) and reduced the amount of non-respirable (systemic drug) and consequently adverse effects (Crompton, 2006).

Various formulations containing different lactose products produced similar ($P > 0.05$) RD (384.0 ± 36.8 μg), similar ED (349.5 ± 33.9 μg), and similar RE (79.8 ± 7.6%) of SS upon aerosolisation (Table 2). The constant weigh of all metered doses (33 ± 1.5 mg), high number of capsules used during actuation for each formulation ($n = 10$), and the formation of ordered mixtures of all formulations (Fig. 4) might be responsible for low variations between RD, ED, and RE between all formulations.

Different formulations produced substantially different DL (drug loss) and EM (emission) of SS (Table 2). By comparison, lactose powders with higher D_b and higher D_{tap} produced higher DL (Fig. 8a) and smaller EM (Fig. 8b) of SS upon inhalation. This indicates that powder cohesiveness of lactose products with higher D_b and higher D_t could not be totally overcome during inhalation leading to the formation of aggregates remaining in the capsules and inhaler device.

IL (impaction loss) of SS varied from 52.4 ± 0.0% for GRA-SS formulation to 79.8 ± 1.6% for FLO-SS formulation (Table 2). IL could be related to amounts of SS which is still adhered to carrier surfaces after aerosolisation. These amounts are expected to deposit on the upper airway regions and eventually swallowed where they become systemically absorbed (Gupta and Hickey, 1991).

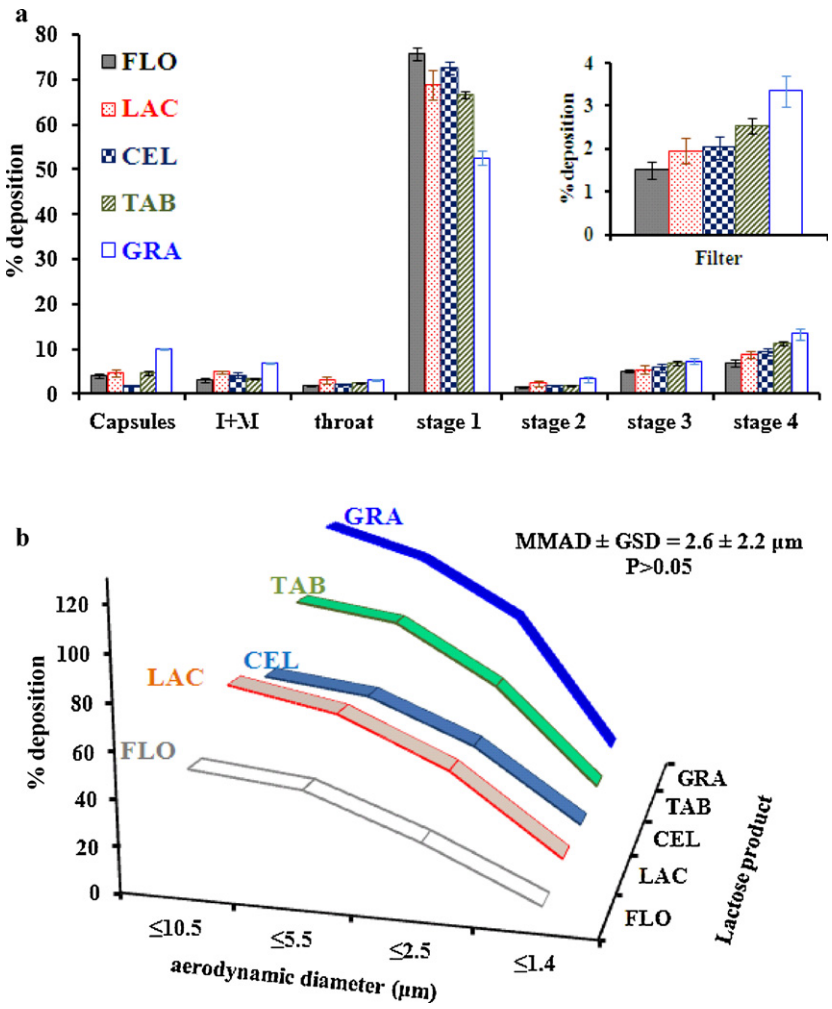

Fig. 7. Amounts of salbutamol sulphate (%, recovered dose) deposited on capsules, inhaler with mouthpiece adaptor (I + M), throat, and different MSLI stages (a); and amounts of salbutamol sulphate (%, recovered dose) (mean ± SE, $n \geq 3$) less than 10.5 μm, 5.5 μm, 2.5 μm, and 1.37 μm aerodynamic diameter (b) obtained after aerosolisation of formulations containing different 63–90 μm sieved lactose products: *Flowlac® 100* (FLO), *Lactopress anhydrous® 250* (LAC), *Cellactose® 80* (CEL), *Tablettose® 80* (TAB), and *Granulac® 200* (GRA). MMAD: mass median aerodynamic diameter; GSD: geometric standard deviation.

EI (ranging from 32.6 ± 3.7% to 47.8 ± 1.1%), DS (ranging from 12.4 ± 2.5% to 32.8 ± 2.1%) and FPD (ranging from 44.8 ± 9.0 μg to 106.0 ± 3.2 μg) were shown to follow a similar rank order according to lactose product as follows: GRA > TAB > CEL ≈ LAC > FLO (Table 2).

All formulations produced similar ($P > 0.05$) MMAD (2.6 ± 0.2 μm) and GSD (2.2 ± 0.1) of SS which indicate that all SS particles are theoretically expected to deposit on lower airway regions giving raise to FPF of 100%. Nevertheless, FPF ranged from 11.5 ± 2.5% for FLO-SS formulation to 27.4 ± 1.5% for GRA-SS formulation (Table 2). Increased FPF variability for FLO-SS and LAC-SS formulations (Table 2) could be partially attributed to reduced drug content homogeneity (higher % CV) within these formulations (Fig. 5). Low FPF (11.5 ± 2.4%) despite high EM (92.6 ± 1.4%) in case of FLO-SS formulation indicates that SS dispersed well from the capsules and inhaler device but could not detach easily from FLO surfaces during inhalation.

In theory, FPF refers to the percentage fraction of the drug which will be locally pharmacologically active in the lung (Dunbar et al., 1998). Higher FPF indicates higher amounts of SS would be expected to be delivered to lower airway regions where SS receptors are mainly located (Labiris and Dolovich, 2003).

Based on this, it can be concluded that FLO carrier produced the poorest aerosolisation performance of SS whereas best DPI aerosolisation of SS was obtained in case of GRA carrier. In theory, improved performance of a DPI formulation could be attributed to either less drug–drug cohesion or less carrier–drug adhesion.

Table 2
Recovered dose (RD), emitted dose (ED), recovery (RE), emission (EM), mass median aerodynaic diameter (MMAD), geometric standard deviation (GSD), fine particle dose (FPD), fine particle dose (FPF), impaction loss (IL), drug loss (DL), dispersibility (DS), and effective inhalation index (EI) of salbutamol sulphare obtained from formulation blends containing different 63–90 μm sieved lactose powders: *Flowlac® 100* (FLO), *Lactopress anhydrous® 250* (LAC), *Cellactose® 80* (CEL), *Tablettose® 80* (TAB), and *Granulac® 200* (GRA) (mean ± SE, $n \geq 3$).

	RD (μg)	ED (μg)	RE (%)	DL (%)	EM (%)	IL (%)	DS (%)	EI (%)	FPD (μg)	MMAD (μm)	GSD	FPF (%)
FLO	389.0 ± 4.5	360.2 ± 1.3	80.9 ± 0.9	7.4 ± 1.4	92.6 ± 1.4	79.8 ± 1.6	12.4 ± 2.5	32.6 ± 3.7	44.8 ± 9.0	2.8 ± 0.1	2.2 ± 0.1	11.5 ± 2.4
LAC	402.5 ± 42.0	363.8 ± 38.5	83.7 ± 8.7	9.6 ± 1.3	90.4 ± 1.3	71.9 ± 5.5	17.8 ± 4.4	37.9 ± 4.8	63.8 ± 12.7	2.7 ± 0.1	2.2 ± 0.0	16.1 ± 3.9
CEL	342.2 ± 30.1	321.7 ± 32.4	71.2 ± 6.3	6.1 ± 1.3	93.9 ± 1.3	74.7 ± 2.6	18.6 ± 1.8	40.5 ± 1.6	59.6 ± 4.0	2.6 ± 0.2	2.2 ± 0.1	17.5 ± 1.5
TAB	403.4 ± 27.1	371.0 ± 26.4	83.9 ± 5.6	8.1 ± 0.7	91.9 ± 0.7	69.4 ± 1.2	22.5 ± 0.5	43.6 ± 0.2	83.5 ± 4.6	2.6 ± 0.1	2.2 ± 0.0	20.7 ± 0.3
GRA	386.7 ± 9.4	322.7 ± 10.8	80.4 ± 2.0	16.6 ± 0.8	83.4 ± 0.8	52.4 ± 0.0	32.8 ± 2.1	47.8 ± 1.1	106.0 ± 3.2	2.4 ± 0.6	2.3 ± 0.1	27.4 ± 1.5

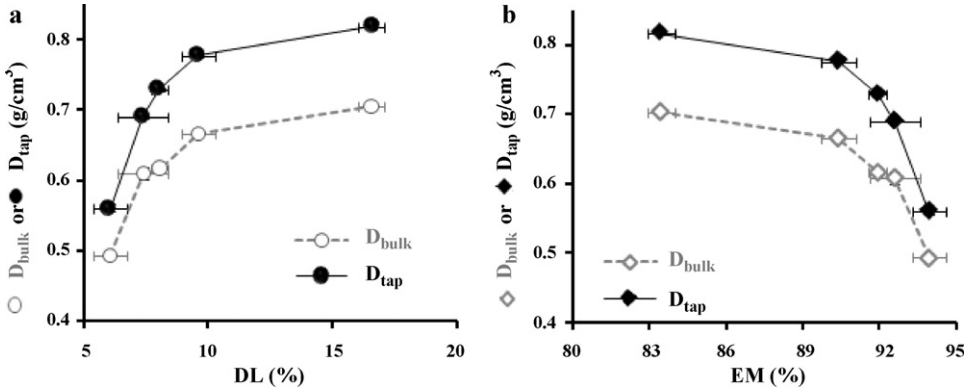

Fig. 8. Drug loss (DL) (a) and emission (EM) (b) (mean ± SE, $n \geq 3$) of salbutamol sulphate in relation to (o) bulk density (D_{bulk}) and (•) tap density (D_{tap}) (mean ± SD, $n \geq 6$) obtained after aerosolisation of formulations containing different 63–90 μm sieved lactose products: *Flowlac® 100* (FLO), *Lactopress anhydrous® 250* (LAC), *Cellactose® 80* (CEL), *Tablettose® 80* (TAB), and *Granulac® 200* (GRA).

However, in this study, both SEM images (Fig. 4) and MMAD data (Table 2) suggest that SS have same degree of cohesion within all formulations. Therefore, differences in SS inhalation properties could only be attributed to different lactose–SS adhesion properties. Strong linear trend ($r^2 = 0.9869$) was established when plotting between FPF of SS against %amounts of SS remained in different formulations after 5 s of functional sieving (Fig. 9a). This confirms that the lower the lactose–SS adhesion forces the higher the amounts of SS delivered to lower airway regions.

Different physical properties between various lactose products may account for different deposition profiles for SS. In case of FLO and CEL, higher adhesion energy is expected, in comparison to other lactose products, due to high amorphous lactose content (Fig. 3; Price and Young, 2005). This might explain poor inhalation properties of FLO-SS and CEL-SS formulations. Also, higher dispersive surface free energy of β-lactose particles (LAC) compared to α-lactose particles (GRA) might explain poor inhalation properties of LAC-SS formulation (Traini et al., 2008).

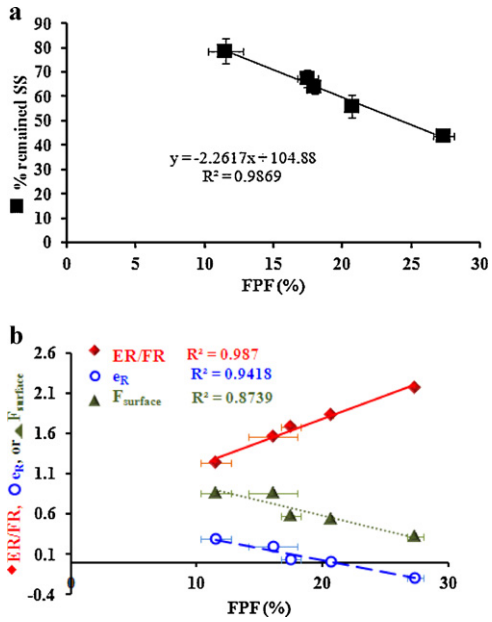

Fig. 9. Relationship between fine particle fraction (FPF) of salbutamol sulphate (SS) (mean ± SE, $n \geq 3$) with (■) % remained SS after 5 s functional sieving time **(a)**; and physical properties of different 63–90 μm sieved lactose products **(b)**: (◆) elongation ratio/flatness ratio (ER/FR), (o) simplified shape factor (e_R), and (▲) surface factor ($F_{surface}$) (mean ± SD, $n \geq 3$).

In comparison to other lactoses, higher ER/FR of GRA particles (Fig. 2) might contribute for enhanced aerosolisation performance of GRA-SS formulation as elongated particles has less stable contact area and thus better deaggregation properties (Otsuka et al., 1988). On the other hand, when the flat region on carrier surface increases, higher degree of carrier–drug adhesion was reported (Iida et al., 2001). Also, comparing to spherical FLO particles (Fig. 2), increased shape irregularity (smaller e_R) and surface roughness (smaller F_{shape}) for GRA particles (Fig. 2) is likely to lead to reduced GRA-SS contact geometry and consequently reduced GRA-SS interparticulate forces resulting in favoured aerodynamic behaviour of SS during inhalation. FPF of SS exhibited linear relationships with respect to lactose ER/FR ($r^2 = 0.987$), e_R ($r^2 = 0.9418$), and $F_{surface}$ ($r^2 = 0.8739$) (Fig. 9b). To further validate DPI performance for different formulations, FPF and lactose physical properties data were analysed in multiple regression and the following equation was generated:

$$\text{FPF} = -15.5 + 35.7(e_R) + 25.0(\text{ER/FR}) - 16.9\,(F_{surface}),\ r^2 = 0.991$$

This indicates that lactose particles with more elongated shape, more irregular shape, and rougher surface produced increased amounts of SS delivered to lower stages of the MSLI (at least within data range of this study). Several studies demonstrated that in vitro aerosolization (FPF) data might correlate well with pharmacokinetic in vivo data (the force vital capacity (FVC), the force expiratory volume (FEV), and the force expiratory flow (FEF)), and could be used to predict drug concentration in patient plasma following inhalation (Lipworth and Clark, 1997; Mitchell et al., 2007; Srichana et al., 2005). However, it should be kept in mind that in vitro measured respirable fraction might overestimate the actual in vivo respirable fraction (Vidgren et al., 1991). For example, in comparison to in vivo results, in vitro aerosolization assessments showed higher amounts of drug deposited on bronchial and alveolar airway regions (Vidgren et al., 1988). This is especially the case in asthmatic patients due to narrow airways (Srichana et al., 2005).

Further investigations would be warranted to compare different sets of carrier commercial grades other than lactose. Also, systemic stability studies would be required to evaluate variations of physicochemical properties and aerosolisation performance of lactose produces when submitted to elevated temperature and humidity.

4. Conclusion

This study offered a comprehensive comparison between different lactose grades in terms of physicochemical properties and DPI performance. After sieving, all lactose grades showed similar particle size distribution and good flow properties. However there

were substantial differences between the lactose grades in terms of their physicochemical properties and the performance of salbutamol sulphate DPI products prepared using the different grades. This study pointed out that the use of milled lactose (Granulac® 200) would be advantageous for pulmonary drug delivery of SS than other lactose products under investigation. This was explained as lactose particles with more elongated shape, more irregular shape, and rougher surface produced increased amounts of SS delivered to lower stages of the MSLI (at least within data range of this study). In addition lower amorphous content observed lead to improved SS delivered to lower stages of the MSLI. The results from this detailed study demonstrate that a good understanding of lactose properties over and above PSD is necessary to make the correct selection and control of lactose grades for pulmonary drug delivery.

Acknowledgements

Waseem Kaialy would like to thank Mr. Ian Slipper (University of Greenwich) and Dr. Ewa Kolosionek (University of Kent) for help provided with SEM images and image optical microscopy, respectively.

References

Bailey, A.G., Hashish, A.H., Williams, T.J., 1998. Drug delivery by inhalation of charged particles. J. Elect. 44, 3–10.
Briggner, L.E., Buckton, G., Bystrom, K., Darcy, P., 1994. The use of isothermal microcalorimetry in the study of changes in crystallinity induced during the processing of powders. Int. J. Pharm. 105, 125–135.
Buckton, G., 1997. Characterization of small changes in the physical properties of powders of significance for dry powder inhaler formulations. Adv. Drug Deliv. 25, 17–27.
Chan, H.K., 2006. Dry powder aerosol delivery systems: current and future research directions. J. Aerosol. Med. 19, 21–27.
Chow, K.T., Zhu, K., Tan, R.B.H., Heng, P.W.S., 2008. Investigation of electrostatic behavior of a lactose carrier for dry powder inhalers. Pharm. Res. 25 (12), 2822–2834.
Crompton, G., 2006. A brief history of inhaled asthma therapy over the last fifty years. Prim. Care Respir. J. 15, 326–331.
Dalby, R.N., Tiano, S.L., Hickey, A.J., 1996. Medical devices for the delivery of therapeutic aerosols to the lungs. Lung Biol. Health Dis. 94, 441–473.
de Villiers, M.M., 1997. Description of the kinetics of the deagglomeration of drug particle agglomerates during powder mixing. Int. J. Pharm. 151, 1–6.
Drapier-Beche, N., Fanni, J., Parmentier, M., 1999. Physical and chemical properties of molecular compounds of lactose. J. Dairy Sci. 82, 2558–2563.
Dunbar, C.A., Hickey, A.J., Holzner, P., 1998. Dispersion and characterization of pharmaceutical dry powder aerosols. Kona 16, 7–45.
Elajnaf, A., Carter, P., Rowley, G., 2006. Electrostatic characterisation of inhaled powders: effect of contact surface and relative humidity. Eur. J. Pharm. Sci. 29, 375–384.
Flament, M.P., Leterme, P., Gayot, A., 2004. The influence of carrier roughness on adhesion, content uniformity and the in vitro deposition of terbutaline sulphate from dry powder inhalers. Int. J. Pharm. 275, 201–209.
Fries, D.C., Rao, S.T., Sundaralingam, M., 1971. Structural chemistry of carbohydrates III. crystal and molecular structure of 4-O-β-D-galactopyranosyl-α-D-glucopyranose monohydrate(α-lactose monohydrate). Acta Cryst. B 27, 994–1005.
Gupta, P.K., Hickey, A.J., 1991. Contemporary approaches in aerosolized drug delivery to the lung. J. Control. Release 17, 127–147.
Hashish, A.H., Fleming, J.S., Conway, J., Halson, P., Moore, E., Williams, T.J., Bailey, A.G., Nassim, M., Holgate, S.T., 1998. Lung deposition of particles by airway generation in healthy subjects: three-dimensional radionuclide imaging and numerical model prediction. J. Aerosol Sci. 29, 205–215.
Harjunen, P., Lankinen, T., Salonen, H., Lehto, V.P., Jarvinen, K., 2003. Effects of carriers and storage of formulation on the lung deposition of a hydrophobic and hydrophilic drug from a DPI. Int. J. Pharm. 263, 151–163.
Hirotsu, K., Shimada, A., 1974. The crystal and molecular structure of β-lactose. Bull. Chem. Soc. Jpn. 47, 1872–1879.
Iida, K., Hayakawa, Y., Okamoto, H., Danjo k. Leuenberger, H., 2001. Evaluation of flow properties of dry powder inhalation of salbutamol sulfate with lactose carrier. Chem. Pharm. Bull. 49, 1326–1330.
Kaialy, W., Momin, M.N., Ticehurst, M.D., Murphy, J., Nokhodchi, A., 2010b. Engineered mannitol as an alternative carrier to enhance deep lung penetration of salbutamol sulphate from dry powder inhaler. Colloids Surf. B Biointerfaces 79, 345–356.
Kaialy, W., Martin, G.P., Ticehurst, M.D., Momin, M.N., Nokhodchi, A., 2010a. The enhanced aerosol performance of salbutamol from dry powders containing engineered mannitol as excipient. Int. J. Pharm. 392, 178–188.
Kaialy, W., Alhalaweh, A., Velaga, S.P., Nokhodchi, A., 2011a. Effect of carrier particle shape dry powder inhaler performance. Int. J. Pharm. 421, 12–23.
Kaialy, W., Martin, G.P., Ticehurst, M.D., Royall, P., Mohammad, M.A., Murphy, J., Nokhodchi, A., 2011b. Characterisation and deposition studies of recrystallised lactose from binary mixtures of ethanol/butanol for improved drug delivery from dry powder inhalers. AAPS J. 13, 30–43.
Kaialy, W., Ticehurst, M.D., Murphy, J., Nokhodchi, A., 2011c. Improved aerosolization performance of salbutamol sulfate formulated with lactose crystallized from binary mixtures of ethanol—acetone. J. Pharm. Sci. 100, 2665–2684.
Kaialy, W., Martin, G.P., Larhrib, H., Ticehurst, M.D., Kolosionek, E., Nokhodchi, A., 2012. The influence of physical properties and morphology of crystallised lactose on delivery of salbutamol sulphate from dry powder inhalers. Colloid Surf. B 89, 29–39.
Kaparissides, C., Alexandridou, S., Kotti, K., Chaitidou, S., 2006. Recent advances in novel drug delivery systems. J. Nanotechnol. Online 2, 1–11.
Kuo, C.Y., Rollings, R.S., Lynch, L.N., 1998. Morphological study of coarse aggregates using image analysis. J. Mater. Civ. Eng. 10, 135–143.
Mitchell, J., Newman, S., Chan, H.K., 2007. In vitro and in vivo aspects of cascade impactor tests and inhaler performance: a review. AAPS Pharm. Sci. Tech. 2007; 8 (4).
Labiris, N.R., Dolovich, M.B., 2003. Pulmonary drug delivery part I: physiological factors affecting therapeutic effectiveness of aerosolized medications. Br. J. Clin. Pharmacol. 56, 588–599.
Larhrib, H., Martin, G.P., Prime, D., Marriott, C., 2003. Characterisation and deposition studies of engineered lactose crystals with potential for use as a carrier for aerosolised salbutamol sulfate from dry powder inhalers. Eur. J. Pharm. Sci. 19, 211–221.
Lipworth, B.J., Clark, D.J., 1997. Effects of airway calibre on lung delivery of nebulised salbutamol. Thorax 52, 1036–1039.
Lefebvre, J., Willart, J.F., Caron, V., Lefort, R., Affouard, F., Danede, F., 2005. Structure determination of the 1/1/mixed lactose by X-ray powder diffraction. Acta Cryst. B 61, 455–463.
Nickerson, T.A., 1974. In: Webb, B.H., Johnson, A.H., Alford, J.A. (Eds.), Lactose. Fundamentals of Dairy Chemistr, 2nd ed. AVI Publishing Co., Westport, CT, pp. 273–324.
Nokhodchi, A., Kaialy, W., Ticehurst, M.D., 2011. The influence of particle physicochemical properties on delivery of drugs by dry powder inhalers to the lung. In: Popescu, M.A. (Ed.), Drug Delivery Book. Nova Science Publishers, Hauppauge, NY, pp. 1–50.
Otsuka, A., Iida, K., Danjo, K., Sunada, H., 1988. Measurement of the adhesive force between particles of powdered materials and a glass substrate by means of the impact separation method III: effect of particle shape and surface asperity. Chem. Pharm. Bull. 36, 741–749.
Platteau, C., Lefebvre, J., Affouard, F., Willart, J.F., Derollez, P., Mallet, F., 2005. Structure determination of the stable anhydrous phase [alpha] lactose from X-ray powder diffraction. Acta Cryst. B 61, 185–191.
Podczeck, F., Newton, J.M., 1994. A shape factor to characterize the quality of spheroids. J. Pharm. Pharmacol. 46, 82–85.
Podczeck, F., Rahman, S.R., Newton, J.M., 1999. Evaluation of a standardised procedure to assess the shape of pellets using image analysis. Int. J. Pharm. 192, 123–138.
Price, R., Young, P.M., 2005. On the physical transformations of processed pharmaceutical solids. Micron 36, 519–524.
Roos, Y., Karel, M.A., 1992. Crystallization of amorphous lactose. J. Food Sci. 57, 775–777.
Smyth, H.D.C., Hickey, A.J., 2005. Carriers in drug powder delivery: implications for inhalation system design. Am. J. Drug Deliv. 3, 117–132.
Srichana, T., Suedee, R., Muanpanarai, D., Tanmanee, N., 2005. The study of in vitro–in vivo correlation: pharmacokinetics and pharmacodynamics of Albuterol dry powder inhalers. J. Pharm. Sci. 94, 220–230.
Staniforth, J.N., 1996. Improvements in dry powder inhaler performance: surface passivation effects. In: Drug Delivery to the Lungs VII. The Aerosol Society, Bristol London.
Taylor, M.K., Ginsburg, J., Hickey, A.J., Gheyas, F., 2000. Composite method to quantify powder flow as a screening method in early tablet or capsule formulation development. AAPS Pharm. Sci. Tech. 1, 20–30.
Telko, M.J., Hickey, A.J., 2005. Dry powder inhaler formulation. Respir. Care 50, 1209–1227.
Todo, H., Okamoto, H., Iida, K., Danjo, K., 2001. Effect of additives on insulin absorption from intratracheally administered dry powders in rats. Int. J. Pharm. 220, 101–110.
Traini, D., Young, P.M., Thielmann, F., Acharya, M., 2008. The influence of lactose pseudopolymorphic form on salbutamol sulfate–lactose interactions in DPI formulations. Drug Dev. Ind. Pharm. 34, 992–1001.
Vidgren, P., Silvasti, M., Vidgren, M., Paronen, P., Tukiainen, H., Lehti, H., 1991. In vitro inhalation behaviour and therapeutic response of salbutamol particles administered from two metered dose aerosols. Pharmazie 46, 41–43.
Vidgren, P., Kärkkäinen, A., Karjalainen, P., Nuutinen, J., Paronen, P., 1988. In vitro and in vivo deposition of drug particles inhaled from pressurized aerosol and dry powder inhaler. Drug Dev. Ind. Pharm. 14, 2649–2665.
Wall, D.A., 1995. Pulmonary absorption of peptides and proteins. Drug Deliv. 2, 1–20.
Zeng, X.M., Martina, G.P., Marriott, C., Pritchard, J., 2000. The influence of carrier morphology on drug delivery by dry powder inhalers. Int. J. Pharm. 200, 93–106.
Zeng, X.M., MacRitchie, H.B., Marriott, C., Martin, G.P., 2007. Humidity-induced changes of the aerodynamic properties of dry powder aerosol formulations containing different carriers. Int. J. Pharm. 333, 45–55.